frontiers in
CELLULAR NEUROSCIENCE

Firing clamp: A novel method for single-trial estimation of excitatory and inhibitory synaptic neuronal conductances

Anton Chizhov, Evgenya Malinina, Michael Druzin, Lyle J Graham and Staffan Johansson

Journal Name:	Frontiers in Cellular Neuroscience
ISSN:	1662-5102
Article type:	Methods Article
Received on:	21 Aug 2013
Accepted on:	08 Mar 2014
Provisional PDF published on:	08 Mar 2014
Frontiers website link:	www.frontiersin.org
Citation:	Chizhov A, Malinina E, Druzin M, Graham LJ and Johansson S(2014) Firing clamp: A novel method for single-trial estimation of excitatory and inhibitory synaptic neuronal conductances. *Front. Cell. Neurosci.* 8:86. doi:10.3389/fncel.2014.00086
Article URL:	/Journal/Abstract.aspx?s=156&name=cellular%20neuroscience&ART_DOI=10.3389/fncel.2014.00086
	(If clicking on the link doesn't work, try copying and pasting it into your browser.)

Firing clamp: A novel method for single-trial estimation of excitatory and inhibitory synaptic neuronal conductances

Anton V. Chizhov[1,*], Evgenya Malinina[2],
Michael Druzin[2,3], Lyle J. Graham[4] and Staffan Johansson[2]

[1] Computational Physics Laboratory, A.F. Ioffe Physical-Technical Institute of the Russian Academy of Sciences, St.-Petersburg, Russia
[2] Department of Integrative Medical Biology, Section for Physiology, Umea University, Umea, Sweden
[3] Department of Neurodynamics and Neurobiology, Lobachevsky State University of Nizhny Novgorod, Nizhny Novgorod, Russia
[4] Neurophysiology & New Microscopies Laboratory, INSERM U603 - CNRS UMR 8154, Université Paris Descartes, Paris, France

Correspondence:
Dr. A.V.Chizhov,
A.F. Ioffe Physical-Technical Institute of RAS,
Politekhnicheskaya str. 26,
St.-Petersburg, 194021,
Russia
anton.chizhov@mail.ioffe.ru

Abstract

Understanding non-stationary neuronal activity as seen *in vivo* requires estimation of both excitatory and inhibitory synaptic conductances from a single trial of recording. We propose a new intracellular recording method for this purpose called “firing clamp”. Synaptic conductances are estimated from the characteristics of artificially evoked probe spikes, namely the spike amplitude and the mean subthreshold potential, which are sensitive to both excitatory and inhibitory synaptic input signals. The probe spikes, timed at a fixed rate, are evoked in the dynamic-clamp mode by injected meander-like current steps, with the step duration depending on neuronal membrane voltage. We test the method with perforated-patch recordings from isolated cells stimulated by external application or synaptic release of transmitter, and validate the method with simulations of a biophysically-detailed neuron model. The results are compared with the conductance estimates based on conventional current-clamp recordings.

Keywords: synaptic conductance estimation, dynamic clamp, firing-clamp

Introduction

Understanding information processing in the brain requires knowledge of neuronal impulse activity and the corresponding synaptic conductance inputs onto target neurons. In particular, phenomena generated by intracortical interactions, including electrical rhythms, waves, and responses to natural or artificial stimulation, could be better understood if the simultaneous

firing activities of excitatory and inhibitory neuron populations were known. Thus, the synaptic conductances arising from these populations, which control the evolution of transmembrane voltage of the target neuron, may provide information on the excitatory and inhibitory neuronal population activities. Estimates of postsynaptic conductances can be obtained from intracellular recordings in a single neuron, but experimental methods of such estimations are still under development, with a principal difference between methods being whether they require repetitive recordings that assume identical input conditions, or not. Given the variability in neuronal responses, even to identical stimuli, single-trial methods are preferable and indeed must be used in some cases, e.g. for evaluation of non-stationary spontaneous activity.

The perhaps most basic method for conductance estimation (Borg-Graham et al., 1998; Anderson et al., 2000; Priebe and Ferster, 2005; Monier et al. 2008; supplementary material S1) implies intracellular measurements of membrane voltage or current at different levels of membrane polarization and thus requires repeatable recordings. In *in vivo* conditions, the method is applied to study evoked responses, when the most important information is contained in signals averaged over several trials. Assuming only two types of synaptic input, thus excitatory and inhibitory, if the averaged traces of voltage or current are recorded at different levels of polarization, and the reversal potentials of both excitatory and inhibitory currents (V_E and V_I) are known, then algebraic calculations provide estimates for the corresponding conductances, G_E and G_I. In the ideal case, it is sufficient to have current records obtained in the voltage-clamp mode at two holding potentials. The difference between the current traces is proportional to the conductance of the target neuron with the difference between the holding potentials as a coefficient. In realistic conditions, the response variability from trial to trial, the contribution of capacitive and voltage-gated currents to the recorded signals etc. reduce the precision of estimation. In a recent paper, Odom and Borisyuk (2012) generalized the current-clamp approach to the case of three estimated synaptic conductances with the help of multiplicative noise, but with the assumption that non-linear channels do not contribute to the recorded voltage traces and the variance of estimated conductance is known *a priori*.

In the case of non-stationary or on-going activity, a single-trial estimation method is required. The most basic method in this case is by periodically perturbing the membrane potential under current clamp with a train of hyperpolarizing current pulses (Douglas et al., 1988). Samples of the cell input conductance are then derived from the corresponding voltage deflections according to a linear model of the cell. This simple approach has two major limitations. First, the repetition rate of the probe current pulses is limited by the resting time constant of the neuron, which typically has an upper bound of tens of milliseconds, corresponding to a maximum sample rate of tens of hertz. For relatively slow synaptic dynamics, for example those underlying up-and-down states (Leger et al., 2005), this rate may be sufficient, but may not be sufficient to measure rapid transient synaptic inputs, for example as seen during visually-evoked activity. In addition, as with the previous current-clamp based methods, a second limitation is that the estimate does not account directly for the non-linear properties of the membrane, in particular when the cell is firing.

Alternatively, a more sophisticated current-clamp method has been proposed by Rudolph et al. (2004), based on the sensitivity of voltage fluctuations, or “noise”, to the input

conductance. In this method the statistical treatment of the recorded membrane voltage is performed with the help of the stationary solution of the Fokker-Planck equation. According to some basic assumptions, this method requires statistically stable states on a time scale of about 100 ms. Thus, for example, the method provides estimates of the up- and down-states of cortical activity *in vivo*, but on the other hand, as above, it is not appropriate for the analysis of faster transient or rhythmic (e.g. theta or gamma range) activity. Similar approaches have been proposed in recent studies (Chizhov and Graham, 2004; Kobayashi et al., 2011). Nevertheless, the question of contamination from spikes and other non-linear responses must still be considered.

The basic principles and limitations of conductance estimation are determined by the control properties of the neuronal membrane. Any synaptically activated ion channel affects the electric activity of the membrane mainly via two mechanisms, shunting and change of polarization due to current. Different synaptic channel types contribute to each of the effects to a different extent, according to their reversal potential and conductance. Their combined effects will determine the total synaptic conductance and total synaptic current. These two signals constitute the principal input signals that control a neuron. This fact is evident from consideration of an equation for membrane voltage, the Kirchhoff's current law (see details in supplementary material S2; Pokrovskii, 1978). If a neuron has an arbitrary set of synapses with voltage-independent conductances and reversal potentials, then the voltage equation contains only two types of terms related to input via synapses or electrode, i. e. terms that are linearly dependent on voltage and terms that are voltage-independent (see Eqs.(A6,A7) in supplementary material S2). The terms of each type determine two linear combinations of input parameters, which control the voltage dynamics. The coefficient of the linearly voltage-dependent term is the total synaptic conductance whereas the voltage-independent term can be referred to as the synaptic current measured at a certain fixed voltage. These two control signals are scalar for one-compartmental and vectorial for multi-compartmental neurons. Because the main assumption requires the synaptic conductances to be voltage independent, such analysis gives only an approximate estimate in the presence of the NMDA-receptor type of glutamatergic channels, which are subject to voltage-dependent block by external Mg^{2+}. Nevertheless, with the above stipulation, the control property described above explains that only two linear combinations of input variables such as the total synaptic conductance and total synaptic current are required to control the voltage. An important consequence following from the given assumptions is that only two input conductances may be estimated using the characteristics of the voltage trace (see also in Odom and Borisyuk, 2012). However, it should be noted that extra assumptions on the temporal characteristics of the synaptic conductances may allow further splitting of the input signals as, for example, in the multi-trial variant of (Odom and Borisyuk, 2012) with extra limitations assumed for the conductance fluctuations.

Simultaneous estimation of two input signals requires conditions in which the voltage evolution is sensitive to changes of current as well as conductance. Such sensitivity is present during spiking, because the mean subthreshold potential is primarily sensitive to the magnitude of current whereas the spike amplitude is more affected by the shunting effect of the total conductance on the depolarization induced by the sodium current, as will be seen from our recordings and simulations. This gives rise to the idea that G_E and G_I may be estimated if the spiking regime could be maintained. The temporal resolution of such estimation will be determined by the frequency of spikes within the train. The precision will

be dependent on the possibilities to minimize the contaminating effects of intrinsic ionic channels, noise, experimental artifacts and synaptic conductance changes between the spikes. Importantly, the most significant of them, the effect of intrinsic ionic channels, might be eliminated if one provides constant interspike interval and after-spike voltage reset, e.g. impose strict initial conditions on the cell prior to each imposed action potential.

To improve the single-trial estimation of synaptic activity, we propose a new quasi-dynamic clamp method that specifically exploits the non-linear dynamics of the action potential. Thus, in lieu of a train of stereotyped hyperpolarizing current pulses, as in the previous single-trial method, here the sample probes are spikes evoked by a train of bi-phasic meander-like current stimuli. The probe spikes are evoked at a constant frequency, and therefore we call the method "firing clamp". Here we describe the method, and present results from electrophysiological recordings of isolated neurons *in vitro*, where conductance responses are evoked by external application or synaptic release of neurotransmitter. In the supplementary material we also present results from numerical simulations of a neuron model for validating the technique.

Methods

Dissociated cell preparation and electrophysiology

Preparation of thin (300 μm) coronal brain slices obtained from young (45 weeks) male Sprague–Dawley rats and mechanical dissociation of medial preoptic neurons from the anterior hypothalamic area as well as composition of extra- and intracellular experimental solutions are described in (Druzin et al., 2011). The extracellular solution, without or with test reagents, was applied by a gravity-fed fast perfusion system. All experiments were carried out at room temperature, 21–23°C. Whole-cell amphotericin-B perforated-patch recordings were made using a Multiclamp 700A amplifier (Molecular Devices, USA) and an acquisition card NI-PCI-6221 (National Instruments, USA) which together with a dual-core Intel processor under Windows XP provided a dynamic clamp time step of 30 μs, using custom software (for details, see http://www.ioffe.ru/CompPhysLab/AntonV3.htm). The injected current was set as $I_{inj}(t)=I(t)-G(t)(V(t)-V_0)$, where $I(t)$ and $G(t)$ are the simulated input current and conductance, respectively, and V_0 is the resting membrane potential. In the firing-clamp regime the current included the meander current, described further below.

"Firing-clamp"

Background protocol. The regime of constant-rate probe-spike firing is set by the injection of a meander-shaped current shown in **Figure 1A,B**, with a rate of 200 Hz. The positive and negative pulse amplitudes depend on the cell admittance and, for the example shown in **Figure 1**, were chosen to be 600 and -400 pA for the neuron with input conductance of approximately 1.5 nS. The positive pulse duration was fixed at 0.81 ms. The negative pulse was maintained until the recorded voltage crossed the fixed reset value -75 mV. We denote the meander current as $I_{Meander}$ (**Figure 1B**).

Calibration. The calibration procedure is aimed to obtain the functions $V^{subthr}(I,G)$ and $V^{pulse}(I,G)$ shown in **Figures 1C,D**. Practically, it is enough to get a few tens of V^{subthr} and V^{pulse} values corresponding to sparsely distributed points (see dots) in a physiologically meaningful domain of the *I*-*G*-plane. The functions $V^{subthr}(I,G)$ and $V^{pulse}(I,G)$ are then obtained by the least-square method as a quadratic polynomial approximation.

Recordings. The target recordings are carried out in the same conditions as during the calibration, i.e. in the presence of meander-like current injection.

Data analysis. At each probe spike *i* of the recorded voltage, $V^{subthr}{}_{\mathrm{i}}$ and $V^{pulse}{}_{\mathrm{i}}$ are measured. The system of equations $V_{\mathrm{i}}^{subthr} = V^{subthr}(I_{\mathrm{i}}, G_{\mathrm{i}})$ and $V_{\mathrm{i}}^{pulse} = V^{pulse}(I_{\mathrm{i}}, G_{\mathrm{i}})$ was then solved using the approximations obtained from the calibration. Considering only excitatory and inhibitory synapses with reversal potentials V_E and V_I, the input signals $(I_{\mathrm{i}},G_{\mathrm{i}})$ are transformed into the synaptic conductances for each probe spike $(G_{E,\mathrm{i}},G_{I,\mathrm{i}})$ as follows (see also supplementary material S2):

$$G_{E,i} = (I_i - G_i(V_I - V_0))/(V_E - V_I), \quad G_{I,i} = G_i - G_{E,i}.$$

Results

As stated in the Introduction, estimation of excitatory and inhibitory synaptic conductances, or equivalently, the input current and conductance, can be performed using probe spikes (**Figure 1B**). To obtain a fixed spike frequency we injected current of a meander-like shape (**Figure 1A**) repeated at a fixed rate, according to the protocol "firing-clamp" described in Methods. Under firing clamp, the initial phase of each meander pattern is comprised of a depolarizing (positive) current pulse of fixed duration (**Figure 1A**), which leads to the suprathreshold activation of sodium channels and a spike. The positive current pulse is then followed immediately by a hyperpolarizing (negative) current pulse, which lasts until the voltage crosses a defined reset value (normally set at -75 mV) (the fact that the duration of this pulse is a function of the measured voltage distinguishes the recording from a strict current-clamp configuration, and thus being formally a dynamic-clamp recording mode). For the remainder of the measurement cycle the injected current is set to zero.

The response to this stimulus pattern provides several conditions for probing the conductance state of the neuron, which constitute the three key ideas of the firing-clamp approach. First, the fast dynamics of the action potential, much faster than the "resting" membrane time constant, allow a rapid sampling rate, e.g. 100-200 Hz. Second, the imposed reset by the hyperpolarizing current pulse ensures that the states of the neuron's fast voltage-dependent sodium and potassium channels are approximately identical at each cycle, as well as allowing a fast spike rate due to an imposed de-inactivation of the sodium channels. Finally, the fixed firing frequency ensures a near constant state for the slow calcium and voltage dependent channels (typically potassium) that underlie spike frequency adaptation under normal firing.

This non-linear method suggests an emphasis on measures that are distinctly sensitive to synaptic current and to synaptic conductance. Thus for our purposes it is convenient to express the total synaptic input in terms of a pure shunting component, $G(t)$, and a pure current component, $I(t)$, the latter measured from the resting potential V_0 (see details in

supplementary material S2;Pokrovskii, 1978). For the case of only two, excitatory and inhibitory synaptic types, the input signals are:

$$G(t) = G_E(t) + G_I(t)$$

$$I(t) = G_E(t)(V_E - V_0) + G_I(t)(V_I - V_0)$$

Note that the $G(t)$ contributes a linear term of the membrane voltage $V(t)$ in the membrane current equation, and that $I(t)$ contributes a term independent of $V(t)$ (see Eqs.(A6,A7) in supplementary material S2).

The spike probes are well suited to estimate the two synaptic components (**Figure 1B**, inset). In particular, the positive pulse response voltage V^{pulse}, defined as the voltage difference at the beginning and end of the positive current pulse, is mainly affected by the shunting effect of the total synaptic conductance. Conversely, the mean subthreshold potential V^{subthr} between spikes after the imposed reset, thus during the inter-meander interval when no current is injected, is primarily sensitive to the magnitude of synaptic current (**Figure 1C,D**). However, these relations are not known a priori for a given neuron. Therefore, before estimating conductance changes from intrinsic synapses, a dynamic-clamp calibration that injects artificial synaptic conductance waveforms to the neuron during quiescent conditions is necessary to estimate the relationships between these voltage measures and the synaptic state:

$$V^{pulse} = V^{pulse}(I,G)$$

$$V^{subthr} = V^{subthr}(I,G)$$

The precision of the estimation depends on the possibility to control the impact of intrinsic ionic channels, with the implicit assumption that the bandwidth of the synaptic conductance changes is consistent with the sampling rate of the spike probes, as well as the standard concerns of noise and experimental artifacts (e.g. due to imperfect electrode compensation). Importantly, the most significant factor, the effect of intrinsic ionic channels, is constrained by enforcing a constant interspike interval and after-spike voltage reset, imposing strict initial conditions on the cell during each measurement cycle.

"Firing clamp" in simulations

To validate the principle underlying the method, we first studied the effects of the stimulation parameters and of noise on the estimation of synaptic input using simulations of a biophysical neuron model, described in the supplementary material (supplementary material S2). In the case of synaptic conductance oscillations at gamma- or theta-range frequencies, the simulations showed that the firing-clamp well splits the excitatory and inhibitory components and reveal the oscillations. The excitatory conductance estimations are quite precise for both, gamma and theta oscillations. The inhibitory conductance estimates tend to be dispersed around the true solution in the shorter time scale case. The method is robust to noise.

"Firing clamp" in experiments *in vitro*

We then tested the firing-clamp method with electrophysiological perforated-patch recordings from dissociated neurons *in vitro*. Current clamp responses of a sample neuron in response to steady and meander-like currents, with and without the application of GABA, are shown in **Figures 1** and **2** (Karlsson et al., 2011). To obtain a fixed spike frequency of the probe spikes

(**Figure 1A**), we injected meander-like current (**Figure 1B**) at a fixed rate of 200 Hz (see Methods). We then measured the values of V^{subthr} and V^{pulse} for each probe spike (**Figure 1B**, inset).

To solve the reverse problem of estimating the synaptic input from the measured values of V^{subthr} and V^{pulse}, the dependence of these variables on I and G was determined by the calibration procedure (**Figure 1C,D**) described above, during which a slow oscillating "synaptic" input conductance was generated in the dynamic-clamp recording configuration. The dynamic-clamp current $I_{inj}(t)$ was calculated as:

$$I_{inj}(t) = I(t) - G(t)(V(t) - V_0)$$

This current was then added to the meander-like stimulus current. Practically, we find that it is sufficient to obtain a few hundred values of V^{subthr} and V^{pulse} corresponding to sparsely distributed points in a physiologically meaningful domain of the *I*-*G*-plane (see dots in **Figure 1C,D**). The global dependencies of V^{subthr} and V^{pulse} on I and G are then approximated by the least-square method as quadratic polynomials.

After recording responses to unknown stimuli, the reverse problem to find I_i and G_i for each pair of measured $V_{subthr,i}$ and $V_{pulse,i}$ values at each probe spike i was accomplished using the approximations obtained by the calibration. Note that the estimations of I_i and G_i are performed without any assumption on the number of synaptic types nor on their reversal potentials. However, the mapping of each estimated pair of I_i, G_i values to the excitatory and inhibitory conductances, G_i^E, G_i^I assumes only two types of receptors with known reversal potentials V^E, V^I. Specifically, we assume that the responses correspond to AMPA and $GABA_A$ receptors, respectively. The values of $G_{E,i}$ and $G_{I,i}$ are obtained as:

$$G_{E,i} = \frac{I_i - G_i(V_I - V_0)}{V_E - V_I}, \qquad (1)$$
$$G_{I,i} = G_i - G_{E,i}.$$

We then recorded responses of the dissociated neurons to the application of GABA and/or glutamate (Glu) (**Figures 2B, 3**). As expected, the estimated GABA-evoked conductance response (**Figure 3A**) consists of a large G_I component without a G_E component (inset), whereas for glutamate-evoked responses (Fig. 3(b)), the G_E component dominates and the G_I component is negligible (see also Suppl. fig. 7 for the analysis of the glutamate response in another cell). Stimulation by a complex sequence of agonist application (Glu, then Glu + GABA, then Glu, as indicated by bars in **Figure 3C**) reveals a prominent excitatory conductance component followed by an inhibitory conductance component, with reduced conductance upon washout of agonists, as expected. During long-lasting application of GABA the reversal potential V_I changes (Karlsson, 2011). We took into account such changes by introducing a variable V_I in Eq.(1), according to the supplementary material S4.

We then estimated the evoked conductances under the same conditions with the continuous current-clamp method on repeated trials at different levels of polarization, described previously. The time course and magnitude of the conductances G_E and G_I estimated by the firing-clamp method compare well to those estimated from the continuous current-clamp method (**Figure 3D,E**). Moreover, the membrane voltage reconstructed from the estimated conductances (**Figure 3F**, dots) is similar to the voltage response recorded in current-clamp mode with no injected current (**Figure 3F**, gray line). Taken together, these results attest to

the consistency of the different methods for the estimation of the synaptic input during application of inhibitory and/or excitatory agonists.

To verify that the firing-clamp method is applicable to rapidly changing synaptic conductances, we then estimated the changes in the synaptic conductances during spontaneous, presumably GABA-mediated, synaptic events (**Figure 4** recorded from different cells than in **Figures 1-3**). We recorded a few synaptic events in firing-clamp mode (**Figure 4A,C)** and, shortly thereafter, in current-clamp mode (Figure 4B,D). The shapes of the estimated inhibitory conductance events are consistent with the shapes of the postsynaptic potentials, demonstrating that the time resolution of the firing-clamp approach is sufficient to reveal isolated synaptic events. In addition, using artificial oscillatory G_E and G_I inputs mimicked by the dynamic clamp, simulations (supplementary material S2) and in *in-vitro* experiments in brain slices (supplementary material S3) demonstrated that the firing-clamp method can reconstruct input conductances changing in the gamma-range frequency.

Discussion

We have developed a new method, the firing-clamp method, for estimating two types of synaptic input to a recorded neuron, in the experiments described here, comprised of glutamatergic input, presumably mediated by AMPA receptors, and GABAergic input, presumably mediated by $GABA_A$ receptors. The method is validated with simulations of a biophysical neuron model, demonstrating that the method performs well with transient and noisy synaptic inputs (see supplementary material S2). Experiments using *in vitro* recordings of isolated neurons and in the brain slice show that the method allows the extraction of inhibitory only, excitatory only, and combined responses to applied synaptic agonists, as well as conductance changes underlying fast spontaneous activity. The (preoptic) neurons studied here are known to express voltage-gated Na^+, K^+ and Ca^{2+} channels and $GABA_A$- AMPA- and NMDA-receptors of types similar to those found in a majority of central neurons. Their detailed biophysical properties, however, vary between cells (c.f. legends to Figs. 3, 4 and Suppl. fig. 7 for the input conductance difference) and also from the model, which was based on hippocampal neurons demonstrating that the firing-clamp method is applicable for any neuronal type. Comparing with the one-trial method from (Rudolph et al., 2004), the bandwidth of the estimated conductances from the proposed firing-clamp is improved by a factor of 20 or more. An alternative single-trial estimation approach from (Paninski et al., 2012) provides a temporal resolution of tens of milliseconds, but has not yet been applied for resolving both excitatory and inhibitory components in experiments.

The sensitivity of the method is due to the fact that the crucial measured characteristics of the probe spikes, V^{subthr} and V^{pulse}, depend on the total synaptic input current measured from rest, I, and the total synaptic conductance, G, in different ways. As shown in **Figure 1C,D**, over much of the relevant range of inputs, V^{subthr} depends mostly on I whereas V^{pulse} is more sensitive on G.

The underlying assumptions limit the applicability of the firing clamp method in its present version to cases when synaptic conductances can be considered as voltage independent. However, further development of the method may be envisaged, for example, introducing a

third characteristic of the probe spikes, sensitive to the known voltage dependence of NMDA-receptor type glutamatergic excitatory synapses.

In conclusion, the proposed method can be used to estimate non-stationary synaptic activity, including single synaptic events, underlying neuronal population interactions and is likely to be useful in *in vivo* conditions for studies of oscillating activity in the gamma or theta range, epileptic discharges etc.

Acknowledgements

The work has been supported by the Russian Foundation for Basic Research (RFBR) with the grant 11-04-01281a, by the Swedish Institute with a short-term visit grant to AVC, by the Swedish Research Council (grant no 22292), by the CNRS and RFBR (Projet International De Cooperation Scientifique grant 4242 to LG and 07-04-92167 to AVC), by the Russian Federal grant 14.B37.21.0852 to MD and by Gunvor och Josef Anérs Stiftelse.

Conflict of Interest Statement

The authors declare that the research was conducted in the absence of any commercial or financial relationships that could be construed as a potential conflict of interest.

Author Contributions

AC worked on method formulation, programming, simulations, experiments and paper writing. MD and SJ did experiments and paper writing. EM did experiments. LG stated the problem and worked on paper writing.

References

Anderson, J. S., Carandini, M., and Ferster, D. (2000). Orientation tuning of input conductance, excitation, and inhibition in cat primary visual cortex. *J. Neurophysiol.* 84, 909–926.

Borg-Graham, L. J., Monier, C., and Fregnac, Y. (1998), Visual input evokes transient and strong shunting inhibition in visual cortical neurons. *Nature* 393, 369–372.

Chizhov, A. V., and Graham, L. (2004). Explanation of shunting effect on membrane potential dispersion, registered in-vivo, by Fokker-Planck equation. *Izvestiya RAEN, ser. MMMIU*, 8, 100-106, in Russian.

Douglas, R. J., Martin, K. A., and Whitteridge, D. (1988). Selective responses of visual cortical cells do not depend on shunting inhibition. *Nature.* 332, 642-644.

Druzin, M., Malinina, E., Grimsholm, O., and Johansson, S. (2011). Mechanism of estradiol-induced block of voltage-gated K^+ currents in rat medial preoptic neurons. *PLoS ONE* 6, e20213.

Karlsson, U., Druzin, M., and Johansson, S. (2011). Cl^- concentration changes and desensitization of $GABA_A$ and glycine receptors. *J. Gen. Physiol.* 138, 609-626.

Kobayashi, R., Shinomoto, S., and Lansky, P. (2011). Estimation of time-dependent input from neuronal membrane potential. *Neural Comput.* 23, 3070-3093.

Leger, J.-F., Stern, E. A., Aertsen, A., and Heck, D. (2005). Synaptic integration in rat frontal cortex shaped by network activity. *J Neurophysiol*. 93, 281–293.

Monier, C., Fournier, J., and Frégnac, Y. (2008). In vitro and in vivo measures of evoked excitatory and inhibitory conductance dynamics in sensory cortices. *J. Neuroscience Methods*. 169, 323-365.

Odom, S.E., and Borisyuk, A. (2012). Estimating three synaptic conductances in a stochastic neural model. *J. Comput. Neurosci.* 32, 191-205.

Priebe, N. J., and Ferster, D., (2005). Direction selectivity of excitation and inhibition in simple cells of the cat primary visual cortex. *Neuron* 45, 133–145.

Paninski, L., Vidne, M., DePasquale B., and Ferreira, D. G. (2012). Inferring synaptic inputs given a noisy voltage trace via sequential Monte Carlo methods. *J. Comput. Neurosci.* 33, 1-19.
Pokrovskii, A. N. (1978). Effect of synapse conductivity on spike development. *Biofizika* 23, 649-653.
Rudolph, M., Piwkowska, Z., Badoual, M., Bal, T., and Destexhe, A. (2004). A method to estimate synaptic conductances from membrane potential fluctuations. *J. Neurophysiol.* 91, 2884–2896.

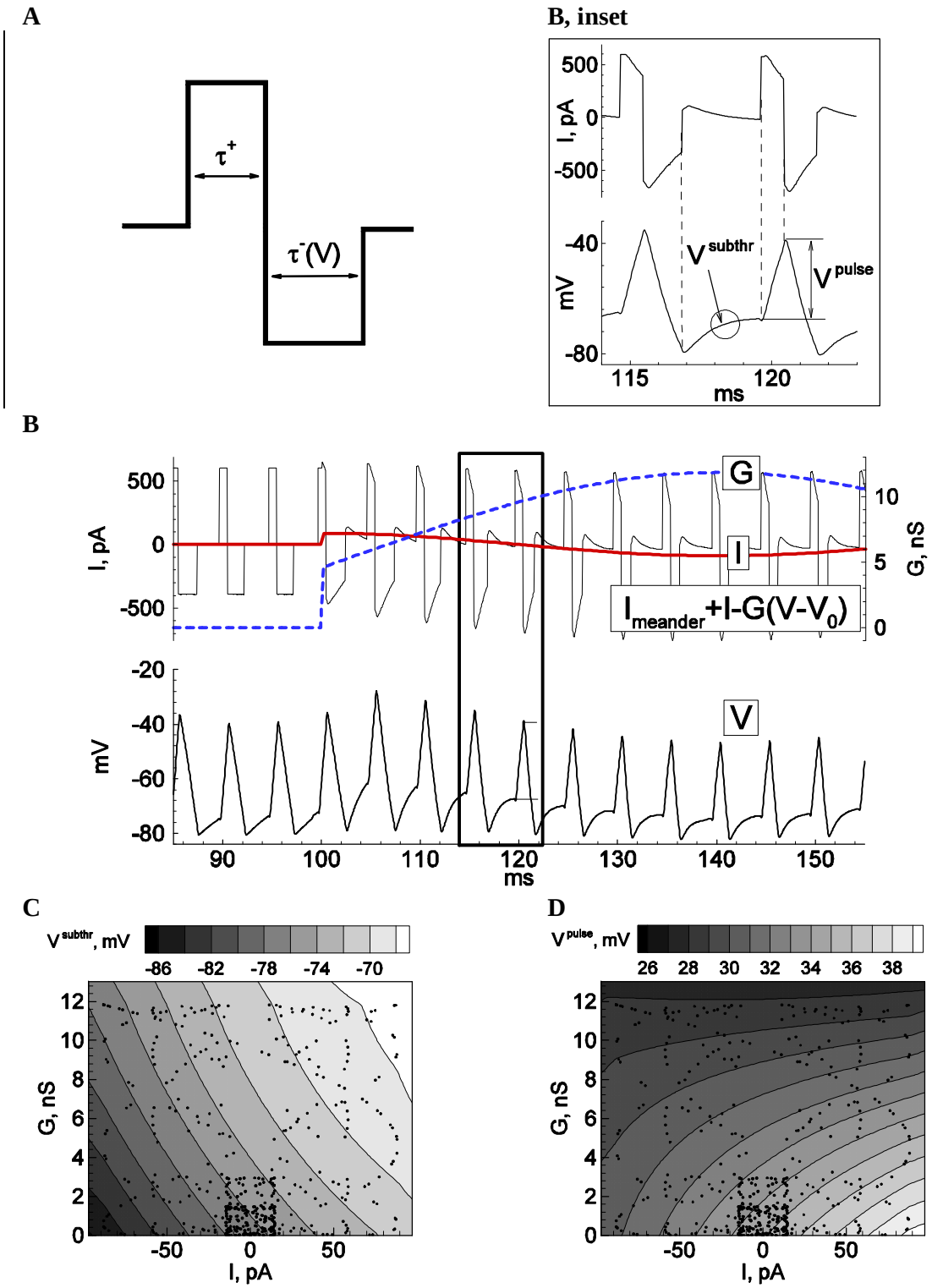
A
B, inset
τ+
τ-(V)
500
0
-500
I, pA
-40
-80
mV
V subthr
V pulse
115
120
ms
B
500
0
-500
I, pA
G
I
I meander+I-G(V-V0)
10
5
0
G, nS
-20
-40
-60
-80
mV
V
90
100
110
120
130
140
150
ms
C
V subthr, mV
-86
-82
-78
-74
-70
12
10
8
6
4
2
0
G, nS
-50
0
50
I, pA
D
V pulse, mV
26
28
30
32
34
36
38
12
10
8
6
4
2
0
G, nS
-50
0
50
I, pA

Figure 1. Principle of firing-clamp technique for conductance estimation: Calibration procedure. Recordings from an MPN neuron were performed in perforated-patch configuration. By means of real-time computer control ('firing-clamp') the voltage-dependent meander-wise current shown in **A** was repeatedly injected at a maintained rate, 200 Hz, which evoked probe spikes (b, bottom). The positive and negative pulse amplitudes of the meander were 0.4 and -0.3 nA, respectively. The positive pulse duration τ^+ was fixed at 0.81 ms, and the negative pulse duration $\tau^-(V)$ was controlled by the recorded membrane voltage, with pulse termination when the voltage reached -80 mV. During calibration, additional sinusoidal current I and conductance G were generated with the dynamic-clamp system, with periods of 40 and 70 ms, respectively. The subthreshold voltage V^{subthr} and the positive pulse response amplitude V^{pulse} were measured for each probe cycle and plotted as functions of the injected I and G. The spikes correspond to dots in **C** and **D**. The functions were approximated by the quadratic polynomials $V^{subthr}(I,G) = 0.002\ I\,G + 0.079\ I + 0.8\ G - 76.8$, and $V^{pulse}(I,G) = -0.0039\ I\,G + 0.0477\ I - 0.49\ G - 34.9$, where voltage, current and conductance are given in mV, pA and nS, respectively.

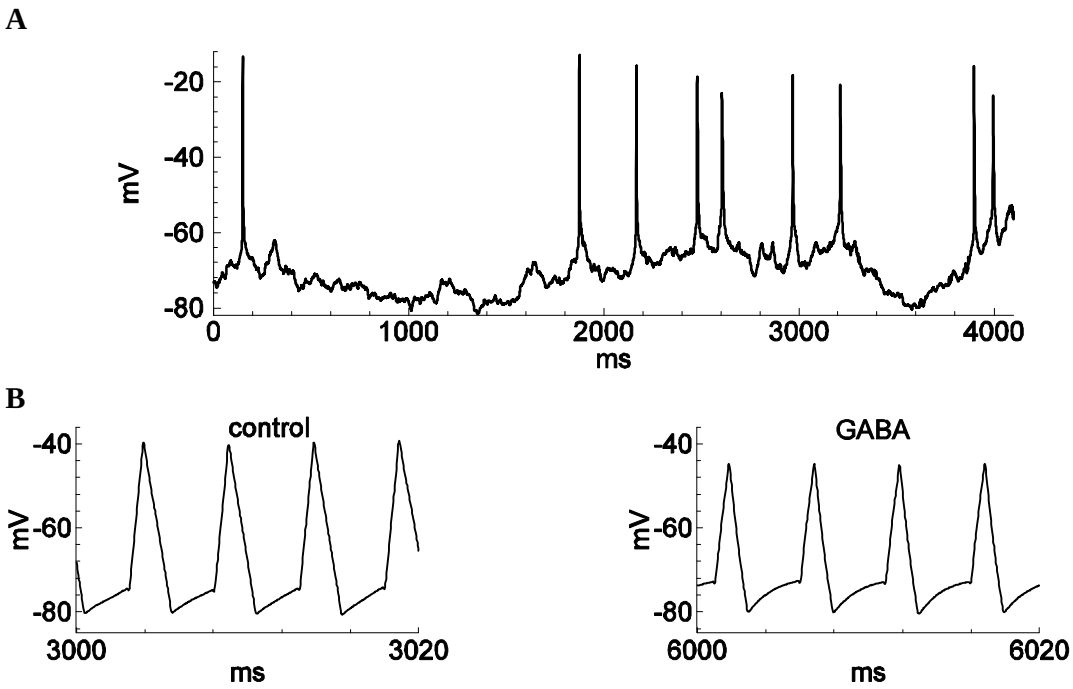

Figure 2. Spontaneous spiking and the activity in firing-clamp regime during GABA application recorded from the same neuron as in **Figure 1**. **(A).** Membrane voltage with occasional spontaneous spikes during hyperpolarizing stimulation by a constant injected current of -30 pA. **(B).** Voltage trace (note expanded time scale) with probe spikes before (left) and during GABA application (1.0 mM; right).

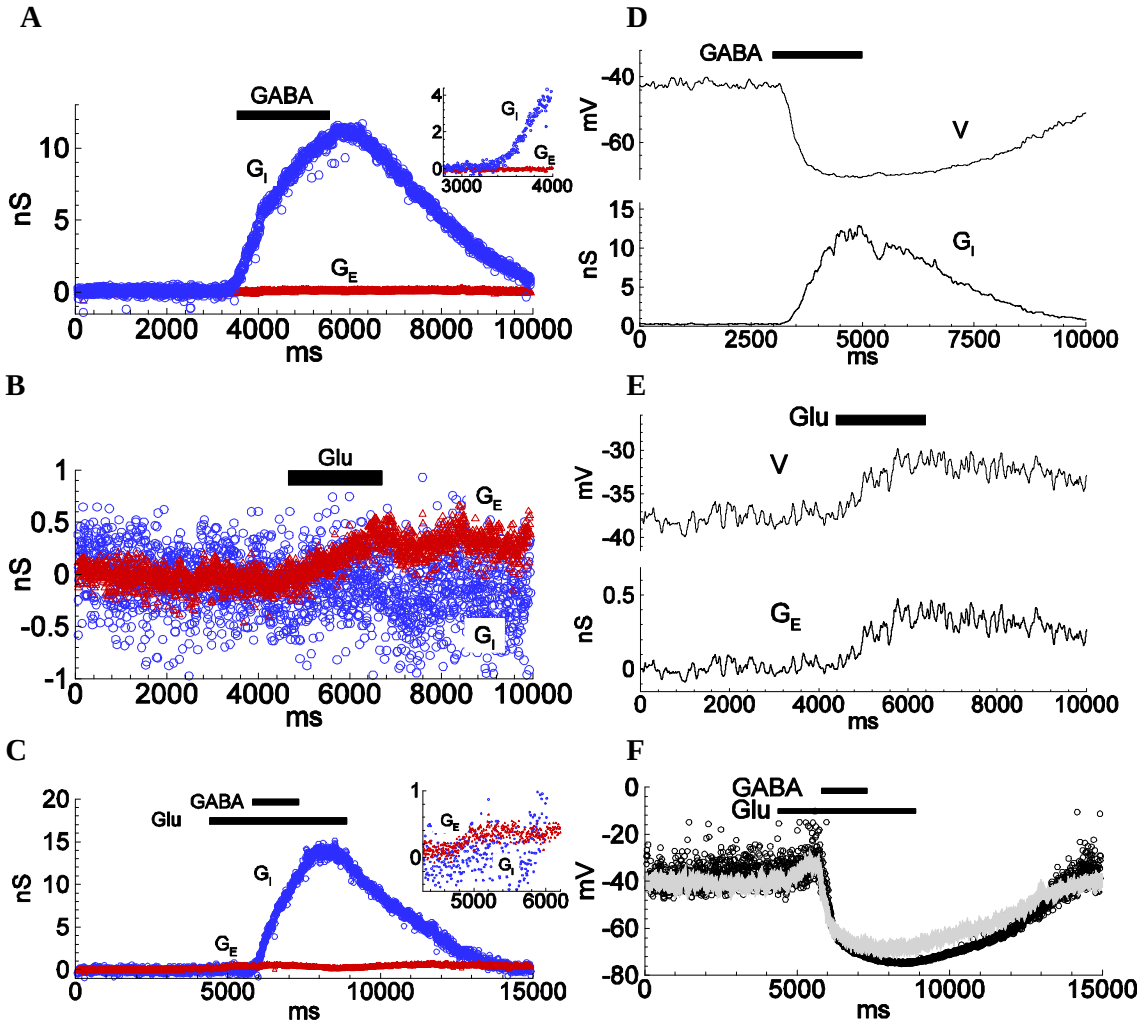

Figure 3. Conductance estimations for responses to applied inhibitory and excitatory agonists using the firing-clamp and the continuous current-clamp methods. **(A,B,C).** Inhibitory and excitatory conductances were estimated by the firing-clamp method from recordings with extracellular application of either GABA (1.0 mM) (**A**; see also **Figure 2**), glutamate (Glu; 1.0 mM) (**B**) or overlapping application of both agonists (c; inset highlights the excitatory component in response to glutamate) Each pair of subthreshold voltage and spike amplitude values evaluated at each probe spike was converted into a pair of excitatory and inhibitory conductances (G_E, G_I), according to the functions shown in **Figures 1C,D**, given reversal potentials V_E = 0 and V_I = -74 mV. **(D, E)**. Conductance estimates (bottom traces in **D**, **E**) from repeated continuous current-clamp recordings of membrane voltage at different holding currents. Inhibitory (**D**, top) and excitatory (**E**, top) voltage responses to application of either GABA (1.0 mM) (**D**) or glutamate (1.0 mM) (**E**). (See supplementary material for the continuous current-clamp technique of estimation, Eqs. S2.3, S2.4). **(F)**. Reconstructed change in membrane voltage from the conductances estimated by the continuous current-clamp method during complex stimulation with glutamate and GABA as in **C**, thus as would be expected in the absence of firing clamp (dots), calculated as $V=(G_0V_0+G_EV_E+G_IV_I)$ /

(G_0+G_E+G_I). Note the similarity to the voltage response to the same type of stimulation as recorded in conventional current-clamp mode with no injected current, (superimposed gray line). All data from the same cell. The input conductance was 1.5 nS. The traces in (**D**, **E**) are low-pass filtered. See Suppl. Fig. 7 for an example of a cell with larger conductance response to applied glutamate.

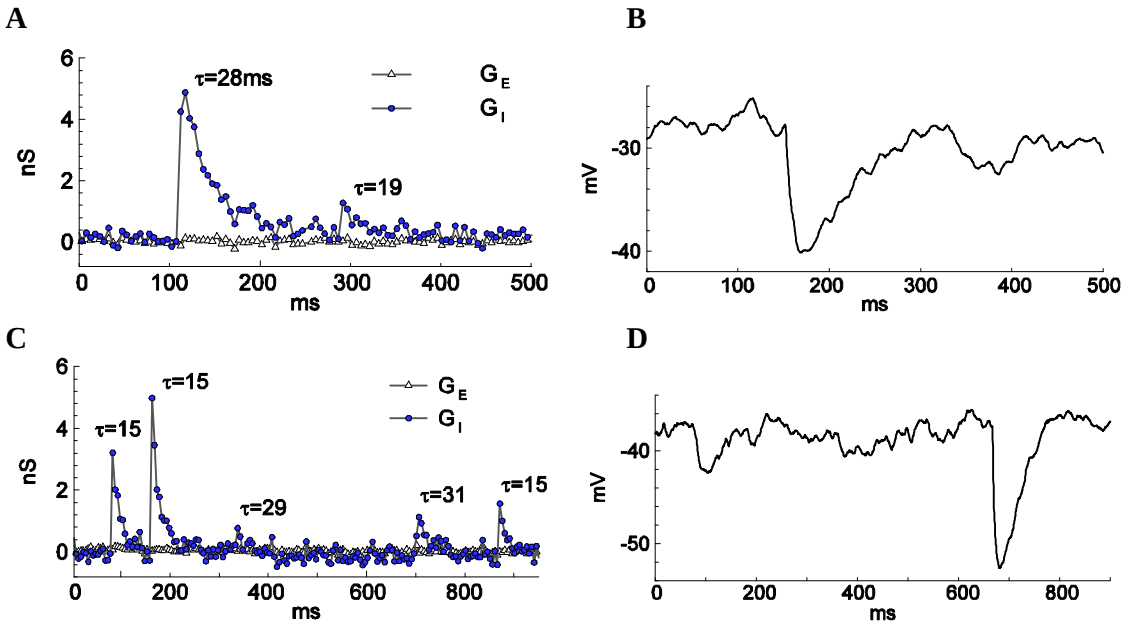

Figure 4. Spontaneous GABA-mediated postsynaptic events of different amplitudes and time courses recorded in firing-clamp (**A,C**) and current-clamp (**B,D**) regimes for two cells (one in A,B and another in C,D) different from the cell of **Figures 1** and **2**. The resting input conductance was 1.6 nS for the cell in A,B and 1.1 nS for the cell in C,D. The time constants (in ms) of mono-exponential fit are given for each event in A and C.

Supplementary material

S1. Multi-trial continuous conductance estimation method in current-clamp mode

The conventional multi-trial method of continuous conductance estimation was originally proposed using the voltage-clamp recording mode by Borg-Graham et al. (1998) and subsequently in modified form using the current-clamp recording mode by Priebe and Ferster (2005). In the current-clamp version, the method uses stimulus-evoked voltage responses that are recorded at two or more levels of injected constant current. It is assumed that the voltage dynamics can be described by a deterministic point-neuron model in the absence of active conductances, allowing the estimation excitatory and inhibitory conductances at each moment in time (thus, determined by the sampling rate of the data acquisition). The voltage-clamp and current-clamp variations have been used in a variety of *in vivo* and *in vitro* studies, for example in the cat visual cortex (Borg-Graham et al., 1998; Priebe and Ferster 2005; Anderson et al., 2000). For the current-clamp approach, the equations written for two measured voltage traces, $V^1(t)$ and $V^2(t)$, corresponding to two levels of holding current (taken here as equal to zero and a non-zero value I), are as follows:

$$-G_E(t)(V^1(t)-V_E)-G_I(t)(V^1(t)-V_I)-G_0(V^1(t)-V_0)=0$$

$$-G_E(t)(V^2(t)-V_E)-G_I(t)(V^2(t)-V_I)-G_0(V^2(t)-V_0)+I=0,$$

where I is the constant current applied when measuring $V^2(t)$. The system of equations gives rise to the estimations:

$$G_I=\frac{-G_0\left[(V^1-V_0)(V^2-V_E)-(V^2-V_0)(V^2-V_E)\right]-I\,(V^1-V_E)}{(V^1-V_I)(V^2-V_E)-(V^2-V_I)(V^2-V_E)}, \qquad \text{(A1)}$$

$$G_E=\frac{-G_0\left[(V^1-V_0)(V^2-V_I)-(V^2-V_0)(V^2-V_I)\right]-I\,(V^1-V_I)}{(V^1-V_E)(V^2-V_I)-(V^2-V_E)(V^2-V_I)} \qquad \text{(A2)}$$

S2. Conductance estimation method “firing clamp” in simulations

Mathematical model of a neuron and its input signals

We consider a conductance-based Hodgkin-Huxley type model of an adaptive hippocampal pyramidal neuron with ionic currents I_{Na}, I_{DR} , I_A , I_H , I_M (Borg-Graham, 1998) and I_{AHP} (Kopell et al., 2000). The calcium-dependent potassium current I_{AHP} provides slow adaptation and the potassium current I_M provides fast adaptation. The explicit formulation of the model can be found in (Chizhov and Graham, 2007). The membrane area is set to $2 \cdot 10^{-5}$ cm^2. The external input may consist of different types of synaptic currents and the current through the electrode I_a, i.e.

$$I_{ext}(t,V) = -\sum_j G_j(t)(V(t) - V_S) + I_a(t), \tag{A5}$$

where G_j is the conductance and V_j is the reversal potential of synapse type *j*. In the main text the case of only G_E and G_I is considered. Here we start from the more general case of arbitrary number of synaptic types.

As noted in (Pokrovskii, 1978), because only V is present in this expression as a state variable of the neuron, we can group the terms into those proportional to V, and free terms, which in turn may be regarded as the two control parameters of the neuron. For convenience, as described in the main text, we introduce these as the total synaptic conductance G and the total synaptic input current I, measured at some arbitrary voltage - as described previously, typically this is taken as the resting potential V_0. The external current may be then rewritten as follows:

$$I_{ext}(t,V) = I(t) - G(t)\,(V(t) - V_0), \tag{A6}$$

where the control parameters are:

$$G(t) = \sum_j g_j(t)$$

$$I(t) = \sum_j G_j(t)(V_j - V_0) + I_a. \tag{A7}$$

Let’s now consider the case of only two types of synapses, excitatory and inhibitory, with the conductances G_E and G_I, and reversal potentials V_E, and V_I. Furthermore, for simplicity we choose $V_I = V_0$, assuming V_0 that is given by the resting potential, which corresponds well with the reversal potential of $GABA_A$ synapses. In this case the control parameters are:

$$G = G_E + G_I\,,\; I = G_E(V_E - V_I)\,. \tag{A8}$$

We use these parameters to construct the method for estimation of the conductances G_E , G_I. The reverse transformation of (I, G) into (G_E , G_I) is:

$$G_E = I/(V_E - V_I)$$

$$G_I = G - I/(V_E - V_I) \tag{A9}$$

Note that this transformation is simpler than the form given in the main text because of the explicit condition that $V_I = V_0$.

Noise

We also tested the firing-clamp method of conductance estimation for robustness in the case of complex, noise-shaped input, by simulating the input conductances as an Ornstein–Uhlenbeck process (Larkum et al., 2004):

$$G_{E,I}(t+dt) = G_{E,I}(t) + \frac{G^0_{E,I}(t) - G_{E,I}(t)}{t}\,dt + s_{E,I}\,x(t)\sqrt{\frac{2\,dt}{t}}, \qquad \text{(A10)}$$

where the time constant τ = *4* ms; the dispersion $\sigma_{E,I}$ relative to the amplitude of the time-dependent mean values $G^0_{E,I}$ is equal to 0.2; and the discretization time step *dt* is 0.05 ms. $x(t)$ is the random number with gaussian distribution, zero mean and unit dispersion. Below, we refer $G_E(t) - G^0_E(t)$ and $G_I(t) - G^0_I(t)$ as to the gaussian colored noise.

Parameters

The stimulus parameters used in the firing-clamp method were then analyzed by using the adaptive neuron model. To obtain spike generation at a constant frequency for a wide range of the control parameters *I* and *G*, the injected current $I_a(t,V)$ included the meander-like pattern shown in **Figure 1A** of the main text with the following parameters: the amplitudes of the positive and negative steps were 800 pA. The duration of the positive step (τ^+) was fixed to 1 ms, with the negative step duration (τ^-) defined by when the membrane voltage crossed the defined reset value of -70 mV. As explained previously, this reset condition fixes the state of the fast membrane channels, including allowing the neuron to fire at a high rate due to fast sodium channel de-inactivation at the reset voltage. The amplitude of the negative pulse must be high enough to finish the repolarization before the fixed start of the next probe spike over the physiologically meaningful range of the inputs *I* and *G*. The frequency of the meander pulses, thus setting the imposed spike interval, was chosen to be 200 Hz, for three main reasons. First, a high frequency is desired to obtain good temporal resolution of the conductance estimation that is commensurate with functionally evoked synaptic inputs. Second, the frequency must also be high enough to avoid "natural" (spontaneous or synaptically evoked) spike generation between the meander-evoked spikes. Finally, the frequency should be low enough to provide time for sodium channel de-inactivation and for integration of the "natural" input current during the interspike intervals, i.e. to provide sensitivity of the voltage to the input current. For most cortical neurons, these constraints imply a frequency range of 80 - 300 Hz. We note that a non-adaptive neuron (e.g. the typical firing characteristic of inhibitory interneurons) can fire at higher rates than a regular-firing (adaptive) neuron (the typical firing characteristic of excitatory neurons), thus implying a higher upper bound for the firing-clamp frequency.

Calibration

Using the adaptive neuron model, we ran a series of simulations over a wide range of the control parameters *G* and *I*, setting these parameters constant for each simulation. We calculated and plotted the subthreshold voltage V^{subthr} and the peak voltage V^{peak} as functions of *(I,* G*),* as shown in **Supplementary figure 1**. The subthreshold voltage V^{subthr} is defined here as the voltage 1.2 ms preceding the peak of the spike (always before the start of the positive pulse) and the peak voltage V^{peak} as the maximum at spike. These definitions allow measurement of the values directly from the voltage curve, and thus do not require precise

synchronization of recorded voltage and current. The time moment 1.2 ms before the spike peak was optimal for the model, in practice providing a reference time just before spike initiation in all regimes. Note that in the experiments the definitions of V^{subthr} and V^{peak} differ from that in simulations. This change for the experiments was made to reduce the impact of artifacts due to non-zero access resistance (i.e. between recording pipette and cytoplasm) and electrode time constant, which appear during abrupt changes of the injected current in the experimental situation.

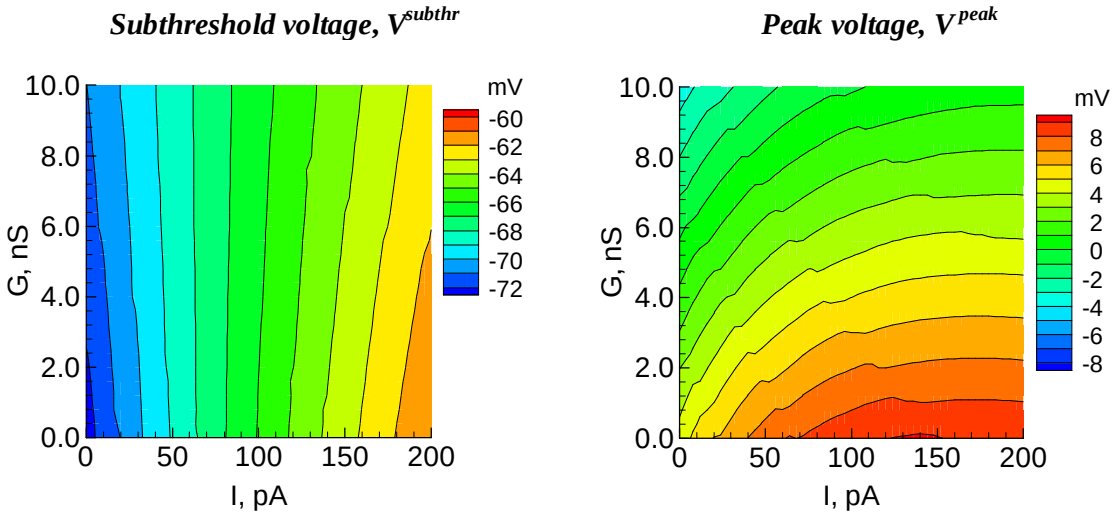

Supplementary figure 1. Dependence of subthreshold voltage and maximum voltage on the control variables *I* and *G* in the steady-state regime of spike generation in the model neuron. The meander-like positive-negative current pulses were applied at 200 Hz. The voltage values were measured at the 80th spike.

"Recordings"

Simulated voltage recordings are obtained by generating different traces of $G_E(t)$ and $G_I(t)$ (i. e. the unknown variables in a biological experiment) and applying the same meander-like current $I_a(t,V)$. We measure two parameters (V^{subthr}, V^{peak}) at each probe spike from a given voltage trace, and find the two control parameters (I, G) as a point corresponding to the intersection of the isolines $V^{subthr}=const$, $V^{peak}=const$ of the two plots. The conductances (G_E, G_I) at every spike are then calculated according to the eqs. (A9).

For the input conductances (G_E, G_I) changing in time as shown in **Supplementary figures 2C,D** by slightly varying (red) and highly varying (green) lines, correspondingly, the voltage curve of the model neuron is shown in **Supplementary figures 2A,B**. Measuring the threshold and peak voltages, we estimate the conductances for the peak-to-peak intervals, shown in **Supplementary figures 2C,D** by the dots. In the presence of the noise modeled according to eq. (A10), the estimations are robust and characterized by similar precision (see **Supplementary figure 2E,F**).

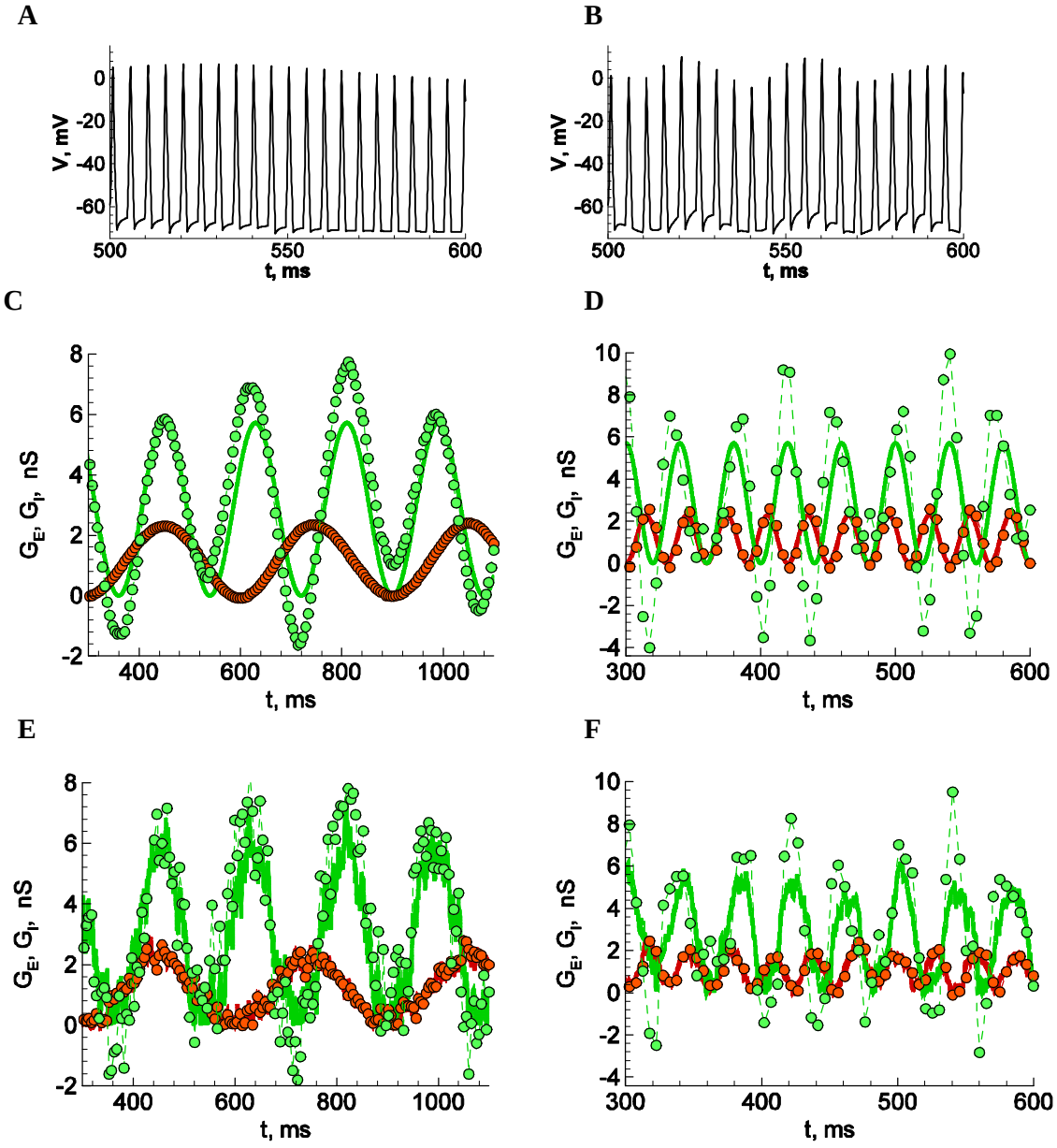

Supplementary figure 2. Estimation of two conductances from "pseudoexperimental" voltage curves. Two examples of excitatory and inhibitory input conductances are shown in **C** and **D** in red and green lines, correspondingly. These input conductances and the injected meander-like current (shown in **Figure 1** of the main text) determine the spike trains shown in **A** and **B**. Estimated points of excitatory and inhibitory conductances are shown by red and green dots, correspondingly. **(E,F).** Estimates in the presence of Gaussian colored noise.

As mentioned, for the experiments we altered the definition of the measured response voltages in order to avoid the contaminating effects of non-zero pipette resistance and capacitance. Specifically, the maximum voltage, V^{peak} was defined as the difference of

potentials measured at the start and at the end of the positive current pulse, thus avoiding electrode artifacts that inevitably follow the abrupt change of injected current. The sub-threshold potential V^{subthr} in the experiments was defined as the mean voltage during inter-meander interval. These variations only slightly affect the estimations.

S3. Estimation of conductances imitated by the dynamic-clamp in a real neuron in a brain slice preparation

To further test the method, we made firing-clamp estimations of artificially injected synaptic conductances supplied by the dynamic-clamp configuration, from a regularly spiking (**supplementary figure 3**) neuron of the rat medial preoptic nucleus recorded in a brain slice preparation.

Methods. The method used has been previously described (Malinina et al., 2010). In short, amphotericin B-perforated patch whole-cell recordings from medial preoptic neurons were made using 150 µm thick acute brain slices from Sprague-Dawley rats and an Axopatch 200B amplifier (Axon instruments, USA). For dynamic-clamp experiments, an acquisition card NI-PCI-6221 (National Instruments, USA) installed in a 2-core Intel processor-based computer running Windows-XP was used. The acquisition card was controlled via custom-built software available at http://www.ioffe.ru/CompPhysLab/AntonV3.htm.

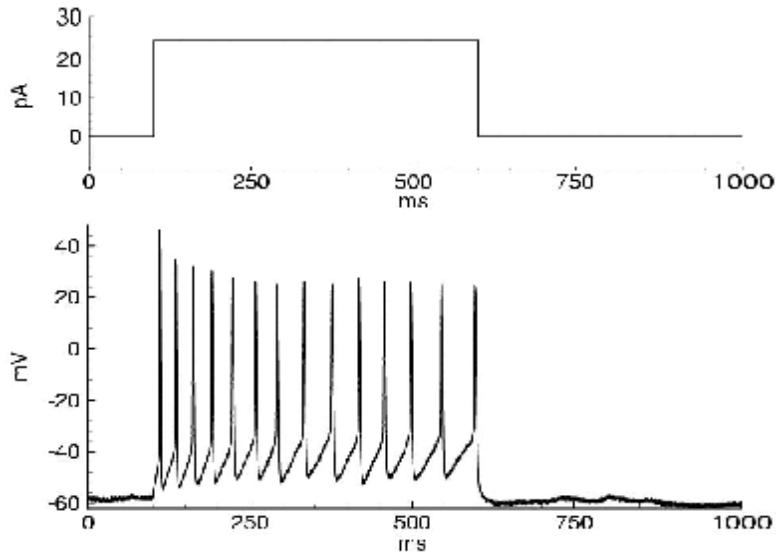

Supplementary figure 3. Impulse activity from a medial preoptic neuron *in vitro*. Voltage response (bottom) to current-step stimulation (top).

"Calibration"

In order to calibrate the firing-clamp method, we measured the functions $V^{subthr}(I, G)$ and $V^{pulse}(I, G)$ by injecting different I and G (**Supplementary figures 4A,B**). To minimize the number of recordings needed for calibration, we limited the calibrations to the voltage responses to three combinations of a step-wise G and a sinusoidal I. Two of these conditions are shown in **Supplementary figures 4A,B**. The calibration data for $V^{subthr,appr.}(I, G)$ and $V^{pulse,appr.}(I, G)$ were approximated by cylindrical functions given in **Supplementary figures 4C,D**.

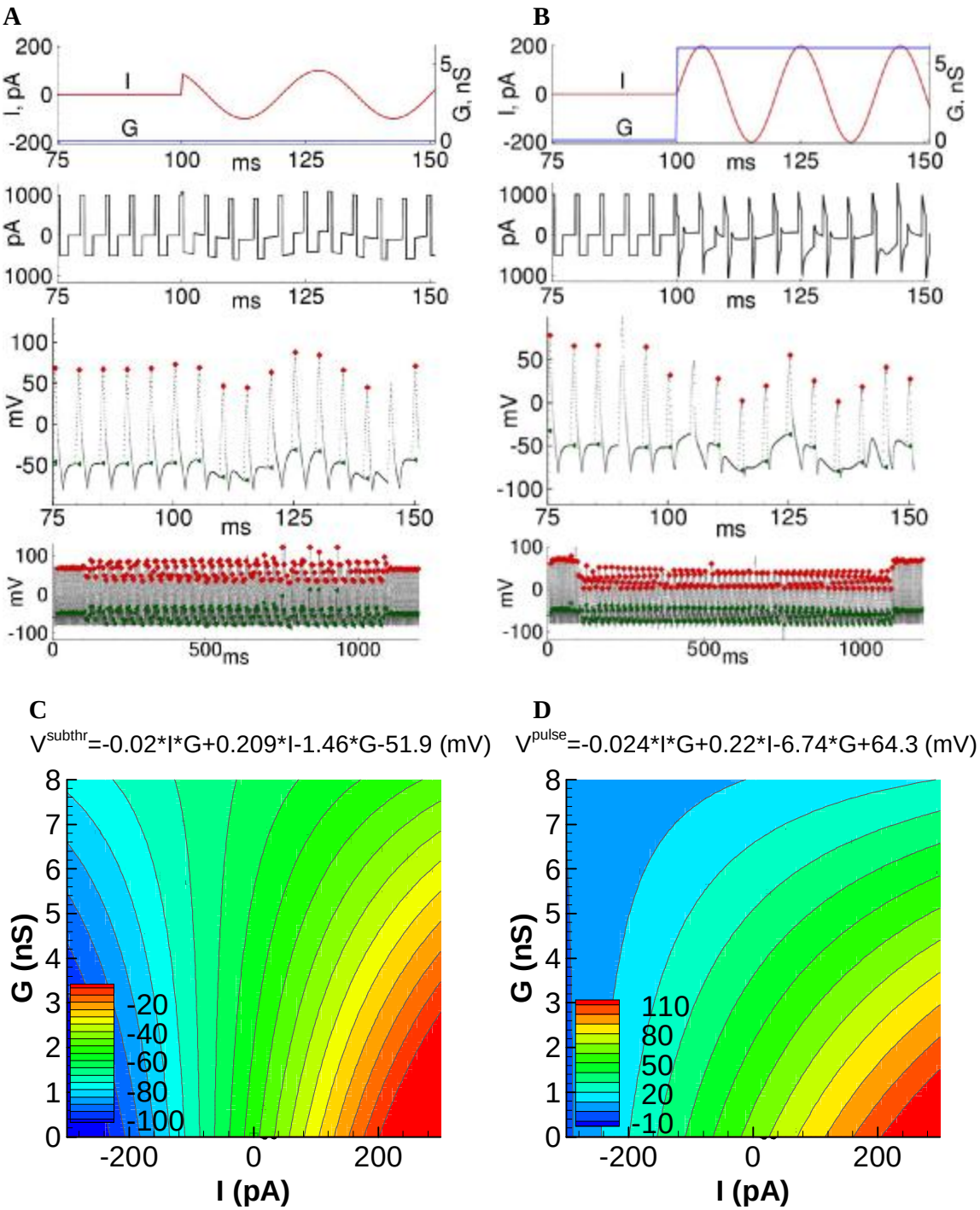

Supplementary figure 4. Calibration records from a medial preoptic neuron *in vitro*. **(A,B)**, Current (2nd from top) and voltage (two lower traces; note different scales for bottom trace) responses to step-wise *G* (top, blue curve in **B**) and sinusoidal *I* (top, red curve) (**A**,**B**). Green triangles denote V^{subthr} and red rhomboids V^{pulse}. Bottom curves plotted in different scale present the whole records used for the calibration. (**C**) and (**D**), approximate plots for V^{subthr} and V^{pulse}, reconstructed from the records shown in (**A**,**B**).

"Recordings"

During firing-clamp recordings with the meander-like stimulus current, we applied an artificially generated "synaptic" conductance step G = 6 nS and a sinusoidal current I of amplitude 400 pA and frequency 30 Hz (**Supplementary figures 5A**, lines) and 10 Hz (**Supplementary figures 5B**, lines), using the dynamic-clamp system. These conductance waveforms were then reconstructed by the estimation method described earlier (triangles in **Supplementary figures 5A,B**, top).

Posteriori estimations

At each probe spike i of the recorded voltage shown in **Supplementary figures 5A,B**, $V^{subthr}{}_i$ and $V^{pulse}{}_i$ were measured. Then, the estimates of I_i, G_i were calculated as the solution of the system of equations $V^{subthr,appr.}(I_i, G_i) = V_i^{subthr}$, $V^{pulse,appr.}(I_i, G_i) = V_i^{pulse}$, using the approximations obtained from the calibration. The corresponding values (triangles) are shown in **Supplementary figure 5**. It is seen that the estimations well correspond to the "true" curves.

A

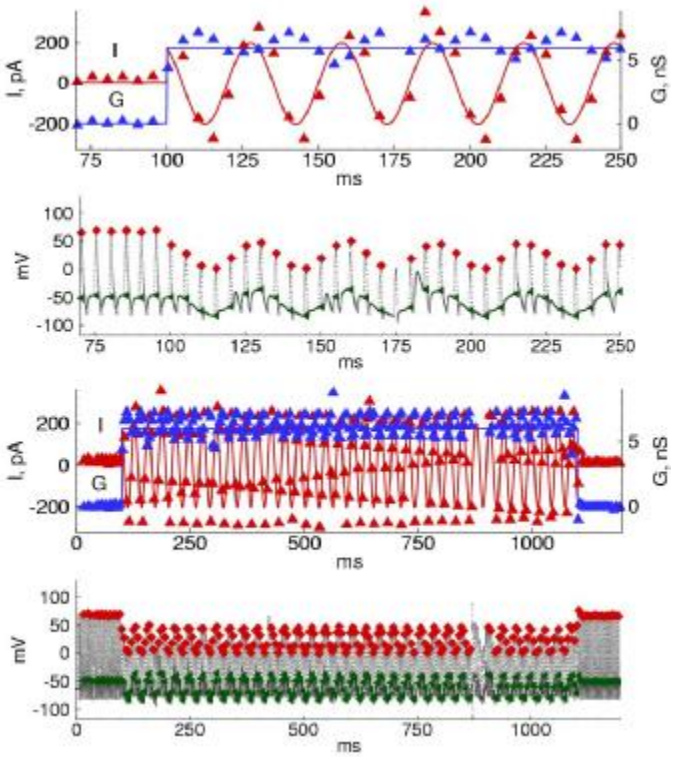

B

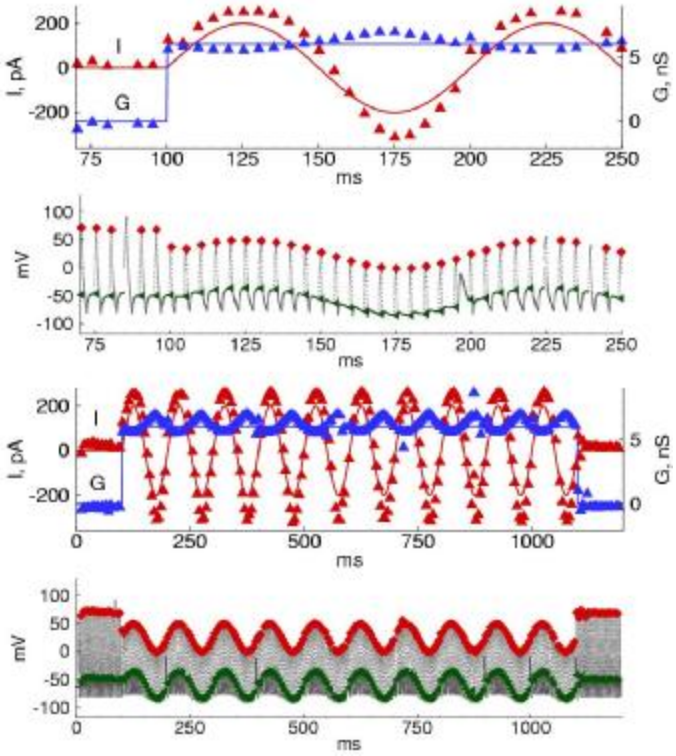

Supplementary figure 5. Recorded data from a medial preoptic neuron in a brain slice preparation. The estimated I and G (red and blue triangles) are compared with the true artificially injected current and conductance (red and blue lines). Recorded voltage curves with the probe spikes are shown as black dotted lines. A step-wise "synaptic" conductance G = 6 nS and a sinusoidal current I with peak-to-peak amplitude 400 pA and frequency 30 Hz (**A**) and 10 Hz (**B**) were applied by the dynamic clamp system. Top two plots in (**A**) and (**B**) show data from the bottom plots at larger magnification.

S4. Evaluation of GABA-ergic reversal potential dynamics

As stated in the main text, whereas the estimation of the total synaptic current I and conductance G does not impose any assumption about the reversal potentials V_E and V_I, the estimation of excitatory and inhibitory synaptic conductances does. The conductances G_E and G_I are obtained from I and G by the formulas (1) of the main text, using certain V_I and V_E. If a synaptic conductance is large, the time course of a synaptic current may significantly alter the corresponding reversal potential, depending on various biophysical properties, including the mechanisms that maintain the concentration gradients of the relevant ions. In particular, this effect may be relevant for the chloride concentration gradient that is the main factor determining the reversal potential of the synaptic current mediated by $GABA_A$ receptors, and, consequently, the estimation of the inhibitory conductance in the present context. In order to account for such factors, we constructed a simple model of the dynamics of the GABA-ergic reversal potential, fitted to the experimental data which allowed a correction for the conductance estimations. Correspondingly, we assume that the synaptic inhibitory current is exclusively composed of chloride ions.

According to Nernst equation and the parameters of our experimental conditions, the reversal potential V_I can be approximated as the chloride reversal potential by the formula:

$$V_I = 25.35 \ln \frac{[Cl]_i}{146} . \tag{1}$$

According to Krishnan and Bazhenov (2011), the chloride concentration dynamics is described by the equation:

$$\frac{d[Cl]_i}{dt} = -\frac{k}{F} I_{Cl} + \frac{[Cl]_i^{\infty} - [Cl]_i}{t_{Cl}} , \tag{2}$$

where $[Cl]_i^{\infty}$ is the initial chloride concentration, F is the Faraday constant, k is the dimensionless coefficient and τ_{Cl} is the time scale. The synaptic inhibitory chloride current is then given by:

$$I_{Cl} = G_I (V - V_I) , \tag{3}$$

where G_I is the GABA-ergic conductance and V is the membrane voltage. In the firing-clamp mode, the main impact of $[Cl]_i$ dynamics to I_{Cl} is during the probe spikes. With respect to the impact on the chloride concentration we assume the shape of the probe spikes to be invariable and that changes of the chloride concentration and inhibitory conductance are much faster than the firing rate. Based on these assumptions, we average the synaptic chloride current over the interspike interval, thus obtaining that I_{Cl} is proportional to G_I with some coefficient k', i.e.

$$I_{Cl}(t) \approx k' G_I(t) . \tag{4}$$

Now, introducing (4) into (2), we obtain:

$$\frac{d[Cl]_i}{dt} = -k'' G_I(t) + \frac{[Cl]_i^{\infty} - [Cl]_i}{t_{Cl}} . \tag{5}$$

The formulas (1) and (5) together describe a simple model of V_I dynamics based on two coefficients k'' and τ_{Cl}. The parameter k'' depends on the firing clamp parameters, whereas the time constant τ_{Cl} depends on the properties of ionic transporters and, in the case of whole-

cell and amphotericin-perforated patch recording, on the equilibration of $[Cl]_i$ with the Cl^- concentration used in the recording pipette.

We find the coefficients k'' and τ_{Cl} from fitting (5) to the estimation of V_I in the case where GABA is applied alone, thus $V_I = V_0 + I/G_I$. In the particular case of **Figures 3A** (main text), the coefficients were $k'' = 0.12\ mM \cdot s^{-1} \cdot nS^{-1}, [Cl]_i^{\infty} = 6.3\ mM$ and $\tau_{Cl}=1\ s$. The time course of G_I and V_I is shown in **Supplementary figure 6**.

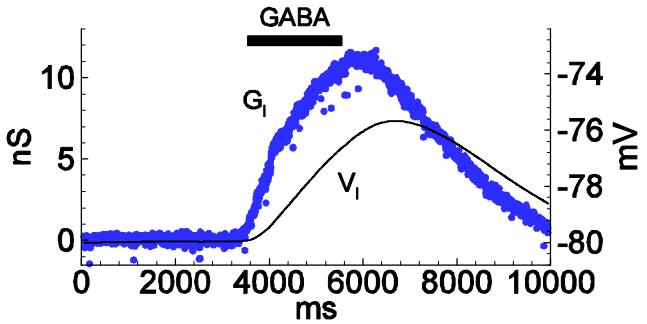

Supplementary figure 6. Estimated inhibitory conductance and inhibitory reversal potential in the case of pure GABA application corresponding to **Figure 3A** of the main text.

S5. Additional example of conductance estimation

Here we present an example of conductance estimations, in addition to those presented in the main text, Figs. 3 and 4. Shown in Suppl. figure 7 is the response to glutamate stimulation for a cell revealing a larger response than that shown in Fig. 3.

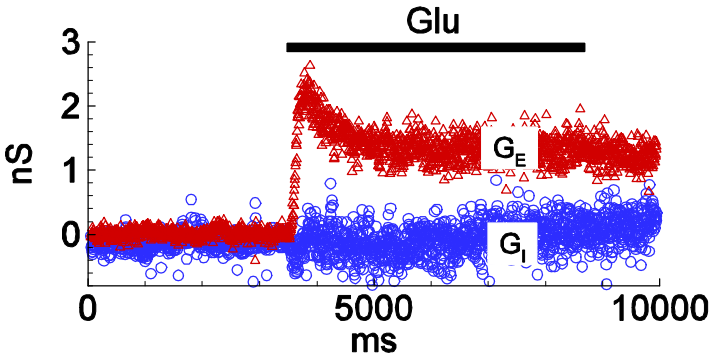

Supplementary figure 7. Estimated evoked conductances in the case of pure glutamate (Glu; 1.0 mM) application. The cell is different from that shown in **Figure 3** of the main text. The resting input conductance of this cell was 0.5 nS.

References

Borg-Graham, L. J., Monier, C., and Fregnac, Y. (1998). Visual input evokes transient and strong shunting inhibition in visual cortical neurons. *Nature* 393, 369–372.

Priebe, N. J., and Ferster, D. (2005). Direction selectivity of excitation and inhibition in simple cells of the cat primary visual cortex. *Neuron* 45(1), 133–145.

Anderson, J. S., Carandini, M., and Ferster, D. (2000). Orientation tuning of input conductance, excitation, and inhibition in cat primary visual cortex. *J. Neurophysiol*. 84, 909–926.

Borg-Graham L. (1998). Interpretations of data and mechanisms for hippocampal pyramidal cell models. In P. S. Ulinski, E. G. Jones, and A. Peters, eds, *Cereb. Cortex*, v.13, pp. 19-138. (Plenum Press, New York).

Kopell, N., Ermentrout, G. B., Whittington, M. A., and Traub, R. D. (2000). Gamma rhythms and beta rhythms have different synchronization properties. *Neurobiology* 97(4), 1867-1872.

Chizhov, A. V., and Graham, L. J. (2007). Population model of hippocampal pyramidal neurons, linking a refractory density approach to conductance-based neurons. *Phys. Rev. E* 75, 011924.

Pokrovskii, A. N. (1978). Effect of synapse conductivity on spike development. *Biofizika*. 23(4), 649-653.

Larkum, M. E., Senn, W., and Lüscher, H.-R. (2004). Top-down dendritic input increases the gain of layer 5 pyramidal neurons. *Cereb. Cortex* 14(10), 1059-1070.

Malinina, E., Druzin, M., and Johansson, S. (2010). Differential control of spontaneous and evoked GABA release by presynaptic L-type Ca^{2+} channels in the rat medial preoptic nucleus. *J. Neurophysiol.* 104(1), 200-209.

Krishnan, G. P., and Bazhenov, M. (2011). Ionic dynamics mediate spontaneous termination of seizures and postictal depression state. *J. Neurosci.* 31(24), 8870-8882.